

# Bidirectional Single-Stage Grid-Connected Inverter for a Battery Energy Storage System

Divya

*mudundi.vaidehi@gmail.com*

*Baba Institute of Technology and Sciences, Visakhapatnam*

**Abstract**—The main objective of this paper is for the battery energy storage system to propose a bidirectional single-stage grid-connected inverter (BSG inverter). This is composed of multiple bidirectional buck–boost type dc–dc converters (BBCs) and a dc–ac unfolder. single-stage power conversion, low battery and dc-bus voltages, pulsating charging/discharging currents, and individual power control for each battery module are the advantages of the proposed BSG-inverter include:. Therefore, the equalization, lifetime extension, and capacity flexibility of the battery energy storage system can be achieved. Based on the developed equations, the power flow of the battery system can be controlled without the need of input current sensor. Also, with the interleaved operation between BBCs, the current ripple of the output inductor can be reduced too. The computer simulations and hardware experimental results are shown to verify the performance of the proposed BSG-inverter.

## I. INTRODUCTION

BECAUSE of the fossil fuel exhaustion and global warming issue, renewable energies such as the photovoltaic (PV) power and wind turbines are more and more popular recently. However, the fluctuations of the high penetration renewable energy will cause the negative impact to the grid voltage and frequency stabilization. A battery energy storage system is a promising candidate to increase the penetration rate of the renewable energy. For the microgrid application, the battery energy storage system is essential not only for controlling and managing the energy of distributed generation units such as PVs, wind turbines, and microturbines for the stability of the power system, but also for protecting loads from grid fault conditions. As shown in Fig. 1, the conventional battery energy storage system consists of a battery array, which is formed by many battery modules connected in series or parallel, and a bidirectional grid-tied dc–ac inverter as a full-bridge inverter [1]–[3]

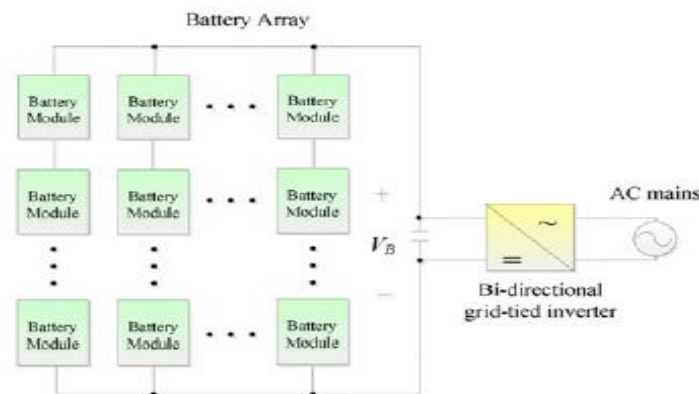


Figure 1. Conventional battery energy storage system

Circuit simplicity is the main advantage of this type of battery energy storage system but the total power capacity may be easily reduced by a particular overcharging/discharging battery module due to the battery tolerance, unequal battery losses, and so on. In order to maximize energy storage, the voltage of the individual battery module connected in series to form a dc bus as the input of the grid-tied inverter must be equalized with each other. The general solution to solve the battery capacity reduction problem is to use extra balancing circuit to connect each battery module and balance the charge of all battery modules. However, the balancing circuit may result in the reduction of total efficiency and the increase of cost and circuit complexity.

## II. PROPOSED BSG-INVERTER

The circuit diagram of the proposed BSG-inverter, which is composed of  $m$  sets of distributed buck–boost type dc–dc converters (BBCs) and a dc–ac unfolder, is shown in Fig. 4. Each BBC consists of two switches, two diodes, and one inductor. It can convert the dc current generated by the battery module into a high frequency pulsating dc current. This high frequency pulsating output current of the BBCs will be converted into sinusoidal one with utility line frequency by the dc–ac unfolder of four active switches operated at low switching frequency and an  $LC$  filter. The proposed BSG-inverter will comply with the power commands, which is coming from the central control unit of the BMS, to charge or discharge the battery modules. The power flow from each battery module is transferred to the ac mains by means of single-stage power conversion. Also, the BBCs can be operated with interleaving to reduce the current ripple of the output inductor.

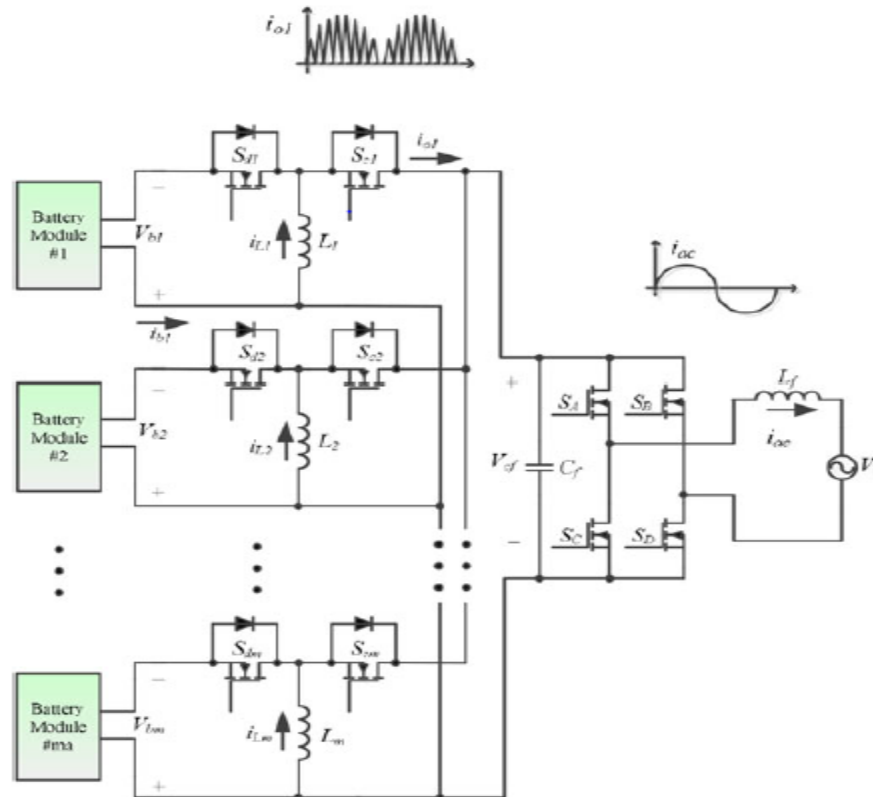


Figure.2 – circuit diagram for the proposed BSG inverter

### A. Discharging Mode Operation

For battery discharging mode of the first BBC set in Fig. 4, the switch  $S_{c1}$  is always turned off and the gate signal of  $S_{d1}$  can be generated by comparing the rectified sinusoidal signal  $V_{sin}$  with the saw-tooth carrier signal  $V_{saw}$  with discontinuous current mode (DCM) operation as shown in Fig. 5(a). Because of the rectified sinusoidal pulse width modulation (SPWM) control with DCM operation, the waveform of the inductor current,  $i_{L1}$ , has an envelope of the rectified ac mains. During the half-cycle of the grid line, the total switching numbers  $N$  can be expressed as follows:

where  $f_s$  is the switching frequency and  $f$  is the grid frequency. Typical waveforms of the inductor current,  $i_{L1}$ , and output current,  $i_{o1}$ , for the DCM operation during the  $k$ th switching cycle are shown in Fig. 5(b)

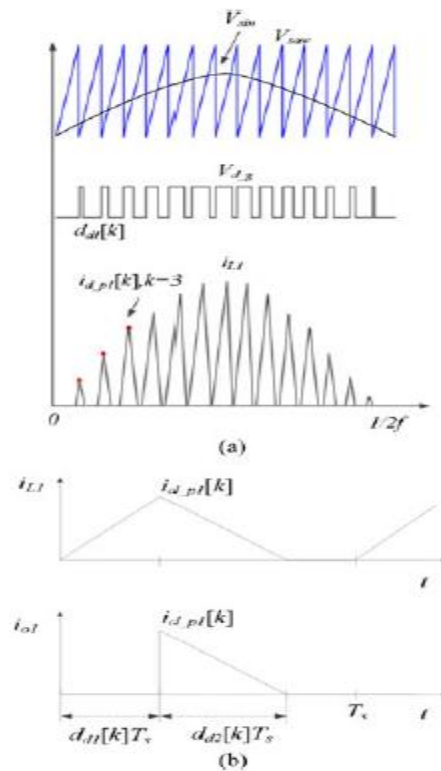
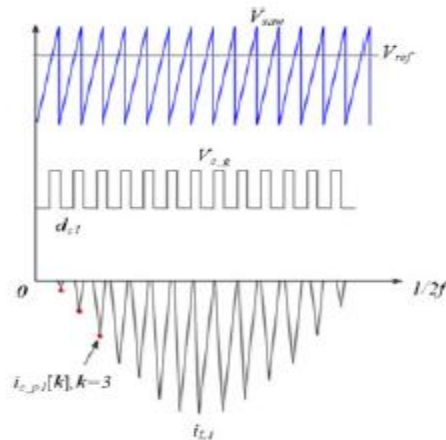


figure.3 - Control signal generation and input inductor current waveform of the first BBC in battery discharging mode. (a) Control signal generation. (b) Typical input inductor current and output current waveforms of the first BBC during the  $k$ th switching cycle

**B. Charging Mode Operation**

For battery charging mode of the first BBC set in Fig. 4, the switch  $Sd1$  is always turned off and the gate signal of  $Sc1$  can be generated by comparing the reference signal  $V_{ref}$  with the saw-tooth carrier signal  $V_{saw}$  with DCM operation as shown in Fig. 6(a). In Fig. 6(b),  $dc1$  is defined as the charging duty ratio of the input inductor  $L1$  and  $dc2 [k]$  is defined as the discharging duty ratio of the input inductor  $L1$  of the  $k$ th switching period  $T_s$ . For the first BBC set, during the charging period of the input inductor  $L1$ , the active switch  $Sc1$  is turned on and the voltage potential across the input inductor  $L1$  is equal to the capacitor voltage  $V_c$  which can be assumed to be the rectified ac mains because of the dc-ac unfolder. When the switch  $Sc1$  is turned off, the voltage potential across the input inductor  $L1$  is reversed and equal to the battery voltage  $V_{b1}$  which results.



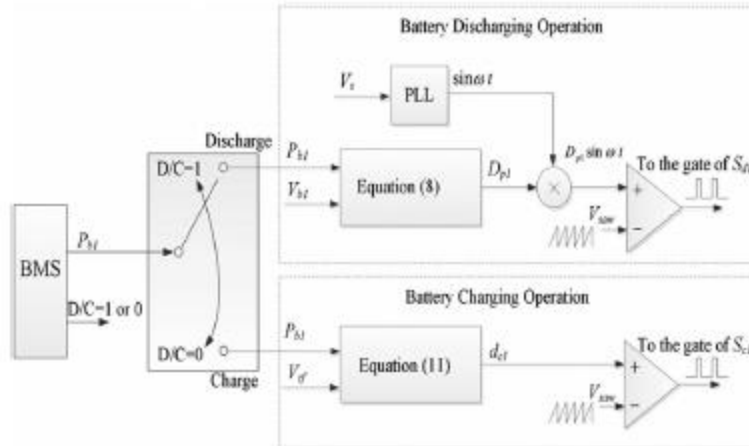


Figure.4 - Control signal generation and input inductor current waveform of the first BBC in battery charging mode. (a) Control signal generation.

Also, the battery charging power can be determined without measuring the battery current. The control block diagram of the first BBC set, as an example, is shown in Fig. 7. The discharging/charging and power commands,  $D/C$  and  $P_{b1}$ , are generated by the BMS and are sent to the controller of the BSG-inverter. The duty cycle signals,  $D_{p1}$  and  $d_{c1}$ , can be determined by using the derived (8) and (11). For the battery discharging operation, the unity sinusoidal function with the grid frequency,  $\sin\omega t$ , can be via a phase-locked loop and is used to obtain the reference signal  $D_{p1}\sin\omega t$ . The gate signal of  $S_{d1}$  can be generated by comparing  $D_{p1}\sin\omega t$  with the saw-tooth carrier signal  $V_{sw}$ . Also, the gate signal of  $S_{c1}$  can be generated by comparing the duty cycle  $d_{c1}$  with the saw-tooth carrier signal  $V_{sw}$  for the battery charging operation. The dc-ac unfold is realized by four active switches operated at low switching frequency and an  $LC$  filter. It can convert the high frequency pulsating dc current generated by the BBCs into a sinusoidal one with utility line frequency. During the positive half-cycle of the ac mains, the switches  $SA$  and  $SD$  are turned-on while  $SB$  and  $SC$  are off. For the negative half-cycle, switches  $SB$  and  $SC$  are ON and  $SA$  and  $SD$  are OFF. Since the unfold is switched at the ac line frequency, its switching loss is very low and can be neglected. Therefore, the proposed BSG-inverter only has one high-frequency PWM signal and can be categorized as a single-stage inverter. For the proposed BSG-inverter, the  $m$ -sets of BBCs can operate in the interleaving fashion. The required synchronization signal for the interleaving operation can be easily obtained from the ac line voltage and no extra communication between BBC is required. By shifting the duty cycles of adjacent channels with  $360^\circ/m$ , the total current ripple of the output inductor can be greatly reduced.

### III. COMPUTER SIMULATIONS AND EXPERIMENTAL RESULTS

A prototype of the proposed BSG-inverter with two BBCs is built and tested. To achieve the desired output power, the component values and parameters must match the equations derived in previous sections. For the 110 Vac,rms/60 Hz utility line, the specifications of the battery modules are listed in Table I. From (4), the maximum duty ratio in battery discharging mode can be obtained

$$D_{p1} < 0.757.$$

From (10), the duty ratio in battery charging mode can also be obtained  $d_{c1} < 0.243$ . (23) The input inductor  $L_m$  as the functions of the switching frequency  $f_s$  can be illustrated in Fig. 10 from (8) and (11). It implies that a small size inductor is possible and the weight of the proposed BSG-inverter can be reduced. However, a high switching frequency implies a large switching loss and the tradeoff between the inductance reduction and the switching loss increment needs to be carefully judged. As shown in Fig. 10, there is no obvious reduction in input inductance when the switching frequency is higher than 20 kHz. Therefore, the switching frequency is selected as 20 kHz for the prototype circuit. From (17) and (21), the maximum output current ripple as a function of  $C_f$  and  $L_f$  is illustrated in Fig. 11. The lower output current ripple implies the larger size of  $L_f$  and  $C_f$ . However, the output capacitor value  $C_f$  is limited by the decrease of the power factor at rated power [17]. Therefore, the tradeoff between output current ripple and the  $LC$  filter size need to be considered while designing BSG-inverter. Based on the derived mathematical equations in previous sections, specifications of the prototype BSG-inverter can be determined as follows.

- 1) Input inductor  $L_1 = L_2 = 180 \mu\text{H}$ .
- 2) Battery module rating voltage  $V_{b1} = 50 \text{ V}$ .
- 3) AC mains =  $110 V_{\text{rms}}/60 \text{ Hz}$ .
- 4) Switching frequency  $f_s = 20 \text{ kHz}$ .
- 5) Output capacitor  $C_f = 2 \mu\text{F}$ .
- 6) Output inductor  $L_f = 1.5 \text{ mH}$ .

With the design procedure presented in pervious sections, the output current of the proposed BSG-inverter can be well controlled. Computer simulations shown in Fig. 12(a) and Fig. 12(b) are the key waveforms of the proposed BSG-inverter for battery discharging and charging operations, respectively. It is obvious that the input inductor current  $i_{L1}$  has an envelope of rectified sinusoidal waveform and an almost sinusoidal output current is generated. In Fig. 12(a), the output current  $i_{ac}$  of the BSGinverter has a peak value equal to 1.5 A in battery discharging mode, where the rms value of the ac mains voltage  $v_{ac}$  is 110 V. In Fig. 12(b), the peak value of output current  $i_{ac}$  is reversed and equal to 1.5 A in battery charging operation.

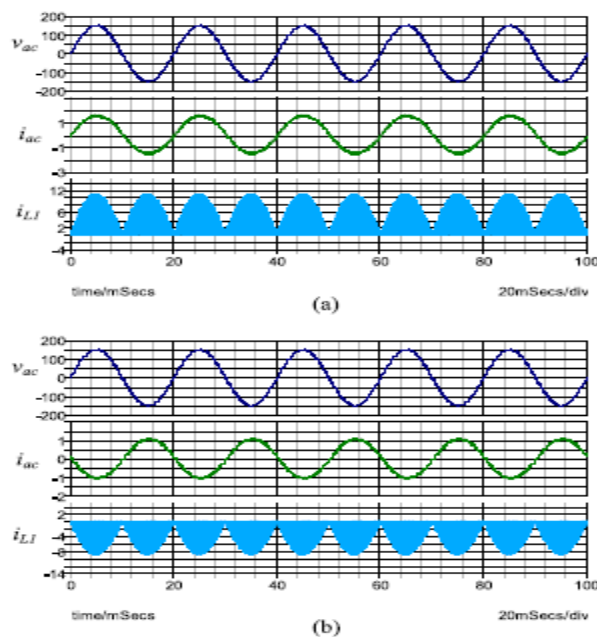


Figure.6 - Computer simulations of ac main voltage (top), ac output current (middle), and input current (bottom) for the BSG-inverter with battery discharging and charging operations. (a) Battery discharging operation. (b) Battery charging operation.

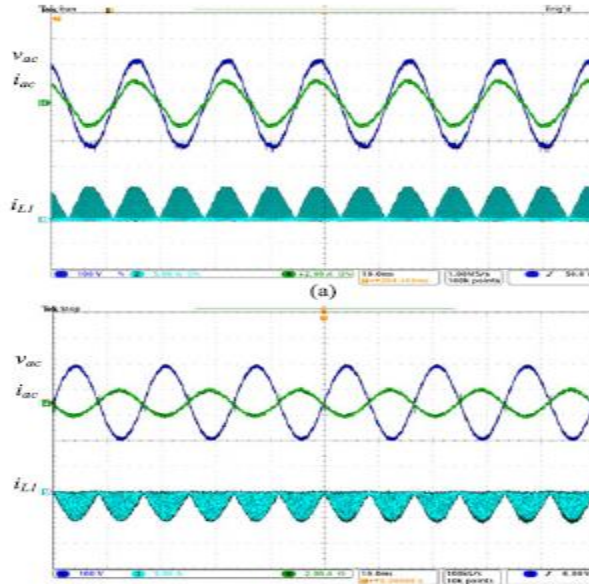


Figure-7 -Experimental waveforms of ac main voltage, ac output current, and input current for BSG-inverter with battery discharging and charging operations. (a) Battery discharging operation. (b) Battery charging operation.

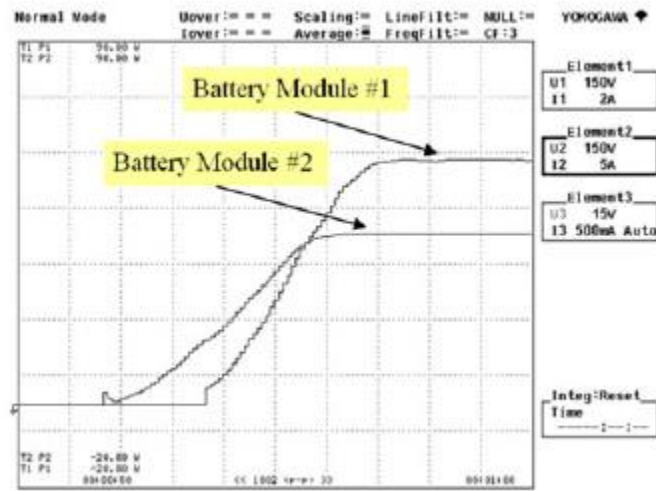


Figure.8 - Measured output power curves of two battery modules with different power commands of the proposed BSG-inverter.

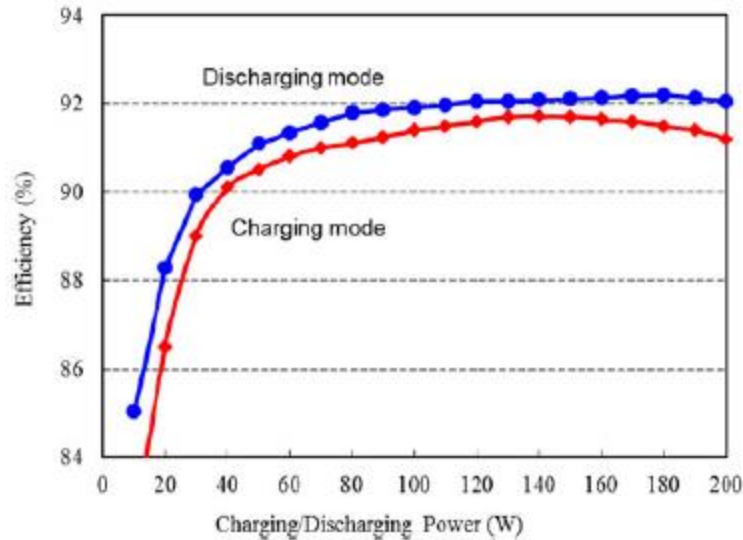


Figure.9- Power conversion efficiency of the proposed BSG-inverter.

#### IV. CONCLUSION

A novel BSG-inverter, which consists of multiple distributed BBCs and a dc–ac unfold, for the battery energy storage system has been proposed in this paper. The proposed BSG-inverter has individual power control capability for each battery module while fulfills the functions of battery charging and discharging by using pulsating current. Eventually, the equalization, lifetime extension, and capacity flexibility of the battery energy storage system can be achieved. According to the developed mathematical equations, the power control capability of each individual battery module can be achieved without the need of input current sensor. Also, with the interleaved operation, the current ripple of the output inductor can be reduced significantly. A design guide line of the proposed BSG is presented. Finally, computer simulations and hardware measurements are shown to verify the validity of the proposed BSG-inverter.

#### REFERENCES

- [1] J. Y. Kim, J. H. Jeon, S. K. Kim, C. Cho, J. H. Park, H.-M. Kim, and K. Y. Nam, "Cooperative control strategy of energy storage system and microsources for stabilizing the microgrid during islanded operation," *IEEE Trans. Power Electron.*, vol. 25, no. 12, pp. 3037–3048, Dec. 2010.
- [2] H. Qian, J. Zhang, J. S. Lai, and W. Yu, "A high-efficiency grid-tie battery energy storage system," *IEEE Trans. Power Electron.*, vol. 26, no. 3, pp. 886–896, Mar. 2011.
- [3] J. He and Y. W. Li, "Hybrid voltage and current control approach for DGgrid interfacing converters with LCL filters," *IEEE Trans. Ind. Electron.*, vol. 60, no. 5, pp. 1797–1809, Mar. 2013.
- [4] M. Y. Kim, C. H. Kim, J. H. Kim, and G. W. Moon, "A chain structure of switched capacitor for improved cell balancing speed of lithium-ion batteries," *IEEE Trans. Ind. Electron.*, vol. 61, no. 8, pp. 3989–3999, Aug. 2014.
- [5] K. M. Lee, Y. H. Chung, C. H. Sung, and B. Kang, "Active cell balancing of Li-ion batteries using LC series resonant circuit," *IEEE Trans. Ind. Electron.*, vol. 62, no. 9, pp. 5491–5501, Sep. 2015.
- [6] W. Huang and A. Qahouq, "Energy sharing control scheme for state-of-charge balancing of distributed battery energy storage system," *IEEE Trans. Ind. Electron.*, vol. 62, no. 5, pp. 2764–2776, May 2015.
- [7] C. L. Chen, Y. Wang, J. S. Lai, and Y. S. Lee, "Design of parallel inverters for smooth mode transfer microgrid applications," *IEEE Trans. Power Electron.*, vol. 25, no. 1, pp. 6–14, Jan. 2010.
- [8] N. Mukherjee and D. Strickland, "Control of second-life hybrid battery energy storage system based on modular boost-multilevel buck converter," *IEEE Trans. Ind. Electron.*, vol. 62, no. 2, pp. 1034–1046, Feb. 2015.
- [9] H. Hu, S. Harb, N. H. Kutkt, Z. J. Shen, and I. Batarseh, "A single-stage microinverter without using electrolytic capacitors," *IEEE Trans. Power Electron.*, vol. 28, no. 6, pp. 2677–2687, Jun. 2013.

[10] N. Sukesh, M. Pahlevaninezhad, and P. K. Jain, "Analysis and implementation of a single-stage flyback PV microinverter with soft switching," *IEEE Trans. Ind. Electron.*, vol. 61, no. 4, pp. 1819–1833, Apr. 2014.